23rd ABCM International Congress of Mechanical Engineering
December 6-11, 2015, Rio de Janeiro, RJ, Brazil

STATE ESTIMATION PROBLEM IN HYPERTHERMIA TREATMENT OF CANCER INDUCED BY NEAR-INFRARED DIODE LASER HEATING

Bernard Lamien
Helcio Rangel Barreto Orlande
Federal University of Rio de Janeiro, PEM/COPPE, CP 68503, Rio de Janeiro, RJ, 21941-972, Brazil
lamienbernard@hotmail.com[1], helcio@mecanica.coppe.ufrj.br[2]

Guillermo Enrique Eliçabe
Inst. Mat. Science and Technology (INTEMA), Univ. Mar del Plata (CONICET) - Mar del Plata, Argentina
elicabe@fi.mdp.edu.ar

Abstract. *In this paper, the hyperthermia treatment of cancer induced by near-infrared laser light is formulated as a state estimation problem and solved with Particle Filters. The physical problem considered in this paper involves the irradiation with a laser in the near infrared range, of a subcutaneous tumor. The tumor is assumed to be loaded with nanoparticles in order to enhance the hyperthermia effects and to limit such effects to the tumor region. The laser tissue interaction is modelled as a coupled radiation-bioheat transfer problem. For the solution of the inverse problem, local temperature measurements are assumed available. The inverse problem involves the estimation of the transient temperature field in the region. Two different Particle Filter algorithms are used in the inverse analysis, namely: the Sampling Importance Resampling (SIR) and the Auxiliary Sampling Importance Resampling (ASIR) algorithms; their performances are compared in terms of accuracy of the inverse problem solution and computational time.*

Keywords: *State estimation, Particle Filter, Hyperthermia, Cancer, Nanoparticles*

1. INTRODUCTION

With the rapid development of computational resources, particle filters have become a very popular class of numerical methods for the solution of Bayesian state estimation problems (Arulampalam et al., 2001, Doucet et al., 2001, Ristic et al., 2004). In such kinds of problems, the available measured data is used together with prior knowledge about the physical phenomena and the measuring devices, in order to sequentially produce estimates of the desired dynamic variables. This is accomplished in a probabilistic framework, so that, the solution of the state estimation problem consists in estimating a posterior probability density through the use of the so-called Bayesian filters (Arulampalam et al., 2001, Doucet et al., 2001, Ristic et al., 2004). Generally, the posterior probability density is not analytically tractable, and Bayesian filters from the Kalman family approximate it with a Gaussian distribution. Unlike these filters, particle filters do not rely on any local linearization or any prior assumption about the posterior probability density (Arulampalam et al., 2001, Doucet et al., 2001, Ristic et al., 2004). Particle filters make use of importance sampling technique, which is a generalization of Monte Carlo approach for the sampling of non-explicit probability densities functions. The posterior probability density, target of the solution of the state estimation problem, is then represented by a set of samples with associated weights, referred as particles (Arulampalam et al., 2001, Doucet et al., 2001, Ristic et al., 2004). It is to be noted that, these features make particle filters method a very useful support for the quantification of uncertainties present in the mathematical formulation of a given physical phenomena as well as in the measurements which might be eventually available. Moreover, one should note that the field of application of Bayesian filters extends from statistics to a broad range of engineering applications, such as, brain imaging, telecommunications, and navigation (Arulampalam et al., 2001, Doucet et al., 2001, Ristic et al., 2004).

Hyperthermia treatment of cancer consists in raising tumor tissues to temperatures between 42-45 ^{o}C during tens minutes. A literature survey shows an increase of survival rates of cancer patients when hyperthermia is used as an adjunctive treatment to radiotherapy or chemotherapy (Hurwitz, 2013). Electromagnetic energy sources like RF and lasers are used to deliver energy to the target region, but they generally lack selectivity, causing damage to healthy tissues. The capacity of conducting nanomaterials like gold nanorods or semi-conducting nanomaterials like carbon nanotubes to serve as strong near-infrared light absorber together with their subcellular size are being explored for a minimally invasive therapy. The rationale is that nanoparticles can be functionalized with specific molecules for targeting actively or passively cancer cells, and then be exposed to an external laser irradiation in order to produce heat locally (Chatterjee and Krishnan, 2013, Bayatoziglu et al., 2013). Although, the use of nanoparticles improves the selectivity of hyperthermia by acting as a local heat source, this treatment generally requires planning or even a predictive model for real-time control in order to minimize damage to normal cells. The overall temperature achieved during the treatment depends on different parameters including tissue properties. It is to be noticed that values available for the optical and thermophysical properties of human tissues present a large variability among patients and physiological states, in addition to uncertainties in tissues geometry; hence, they constitute a considerable source of uncertainties that should be accounted for in the simulations (Lamien et al., 2014, Dos Santos et al., 2009, Greef et al., 2011).

This work aims at the comparison of two particle filter algorithms, namely: the Sampling Importance Resampling (SIR) algorithm and the Auxiliary Sampling Importance Resampling (ASIR) algorithm, for the solution of an inverse heat transfer problem of temperature field estimation resulting from the hyperthermia treatment of cancer, by assuming available local temperature measurements from a single sensor. The temperature field results from the laser heating of a subcutaneous tumor loaded with nanoparticles.

2. PHYSICAL PROBLEM AND MATHEMATICAL FORMULATION

The physical problem under picture in this paper involves the hyperthermia treatment of a subcutaneous tumour, induced by an external collimated plan laser beam under constant illumination (CW) (Çetingül and Herman, 2010, 2011). The skin is represented as an inhomogeneous cylindrical medium with five layers, where each layer corresponds to a specific tissue, namely: epidermis, dermis, fat, muscle and a tumour buried in the dermis (See figure 1). The tumour is assumed to be loaded with gold nanorods in order enhance the hyperthermia effects and to limit such effects to the tumour region.

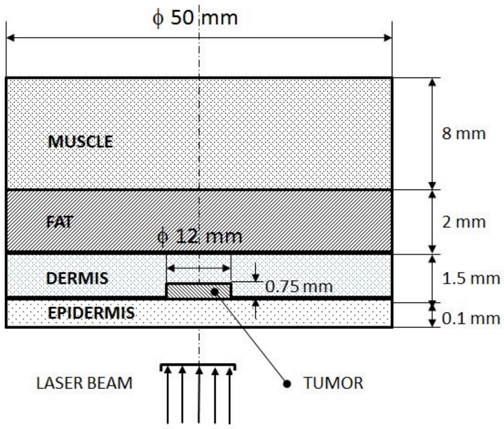

Fig. 1 Sketch of the skin model

The laser radiation propagation in the skin is modelled with the diffusion δ-P1 approximation (Star, 2011, Carp et al., 2004).The laser beam is assumed to be co-axial with the cylindrical skin model, so that the problem can be formulated as two dimensional with axial symmetry. At the external surface of the skin, the incident laser radiation is assumed to be partially reflected (specular reflection), with reflection coefficient R_{sc}. The internal surface of the irradiated boundary is assumed to partially and diffusively reflect the incident radiation, with reflectivity characterized by Fresnel's coefficient A_1, while opacity is assumed for the remaining boundaries. The refractive indexes (n_t) of the different tissues are assumed constant and homogeneous. The mathematical formulation of the radiation problem within the δ-P1 approximation for the problem under study is given hereafter.

The diffuse component of the fluence rate is given by the following boundary value problem (Star, 2011).

$$\nabla\cdot\left[-D(r,z)\nabla\Phi_s(r,z)+\frac{\sigma_s'(r,z)g'(r,z)}{\beta_{tr}(r,z)}\Phi_p(r,z)\right]+\kappa(r,z)\Phi_s(r,z)=\sigma_s'(r,z)\Phi_p(r,z)$$

$$\text{in}\quad 0<r<L_r \quad\text{and}\quad 0<z<L_z \tag{1.a}$$

$$-D(r,z)\nabla\Phi_s(r,z)\cdot\mathbf{n}+\frac{1}{2A_1}\Phi_s(r,z)=-\frac{\sigma_s'(r,z)g'(r,z)}{\beta_{tr}(r,z)}\Phi_p(r,z)\quad \text{at } z=0,\ 0<r<L_r \tag{1.b}$$

$$\Phi_s(r,z)=0 \qquad \text{at } z=L_z,\ 0<r<L_r \tag{1.c}$$

$$\nabla\Phi_s(r,z)\cdot\mathbf{n}=0 \qquad \text{at } r=0,\ 0<z<L_z \tag{1.d}$$

$$\Phi_s(r,z)=0 \qquad \text{at } r=L_r,\ 0<z<L_z \tag{1.e}$$

where

$$D=\frac{1}{3\beta_{tr}}\ ;\ \sigma_s'=\left(1-g^2\right)\sigma_s\ ;\ g'=\frac{g}{1+g}\ ;\ A_1=(1+R_2)/(1-R_1)\ ;\ \beta_{tr}=\kappa+\sigma_s(1-g) \tag{2.a-e}$$

with g being the anisotropy factor of scattering, σ_s the scattering coefficient, while R_1 and R_2 are the first and second moments of Fresnel's reflection coefficient, respectively.

The collimated component of the fluence rate follows the generalized Beer-Lambert's law and is given by (Star, 2011):

$$\Phi_p(r,z)=\Phi_{0,i}(r,z)=\Phi_{0,i-1}\left(r,d_{i-1}(r)\right)\exp\left[-\beta_i'(z-z_i)\right] \tag{3.a}$$

with

$$\beta'=\kappa+\sigma_s' \tag{3.b}$$

where the subscript i refers to the layer i, d_i is the thickness of each layer, while z_i and $\Phi_{0,i-1}$ are the axial position at which the collimated light enters layer i and the collimated fluence rate at this position, respectively. For i = 1 we have:

$$\Phi_{0,1}(r,z)=(1-R_{sc})E(r)\exp(\beta_1'z) \tag{3.c}$$

with

$$E(r)=\begin{cases}E_0, & r\le L_{tumor}\\ 0, & r>L_{tumor}\end{cases} \tag{3.d}$$

The total fluence rate is obtained by adding both diffuse and collimated components, that is,

$$\Phi(r,z)=\Phi_p(r,z)+\Phi_s(r,z) \tag{4}$$

The heat transfer problem resulting from the laser irradiation of the medium is modelled in terms of the two-dimensional bioheat transfer equation in cylindrical coordinates with axial symmetry. The internal surface (at $z = L_z$) is assumed to exchange heat with the deeper tissues with a convective heat transfer coefficient h_{int}, while the irradiated surface (at z = 0) is assumed to be cooled by air in order to avoid overheating of the skin (Dombrovsky et al., 2012). The heat transfer coefficient and the temperature of the surrounding medium at z = 0 are assumed to vary in the radial direction. Heat transfer is neglected through the lateral surfaces of the medium. The heat transfer problem is then formulated by using position-dependent properties as:

$$\rho(r,z)c_p(r,z)\frac{\partial T(r,z,t)}{\partial t}=\nabla\cdot\left[k(r,z)\nabla T(r,z,t)\right]+Q(r,z),\quad 0<z<L_z\ ,0<r<L_r\quad t>0 \tag{5.a}$$

$$k(r,z)\nabla T(r,z,t)\cdot\mathbf{n}+h_c(r)T(r,z,t)=h_c(r)T_c(r)\quad ,\quad z=0\quad ,0<r<L_r\quad t>0 \tag{5.b}$$

$$k(r,z)\nabla T(r,z,t)\cdot\mathbf{n}+h_{\text{int}}T(r,z,t)=h_{\text{int}}T_{\text{int}}\quad ,\quad z=L_z\ ,\ 0<r<L_r,\ t>0 \tag{5.c}$$

$$\nabla T(r,z,t)\cdot\mathbf{n}=0\quad ,\quad r=0\quad ,0<z<L_z\quad t>0 \tag{5.d}$$

$$\nabla T(r,z,t)\cdot\mathbf{n}=0\quad ,\quad r=L_r\quad ,0<z<L_z\quad t>0 \tag{5.e}$$

$$T(r,z,t)=T_s(r,z)\quad 0<z<L_z\ ,0<r<L_r,\quad t=0 \tag{5.f}$$

where

$$Q(r,z)=\rho_b c_{p,b}\omega_b(r,z)\left[T_b-T(r,z,t)\right]+Q_{met}(r,z)+Q_{laser}(r,z) \tag{5.g}$$

The heat source term given by equation (6.a) includes the heat source due to laser absorption,

$$Q_{laser}(r,z) = \kappa(r,z)\Phi(r,z) \tag{5.h}$$

but also the heat source due to metabolism and the effect of blood perfusion. The heat source term Q_{laser} induced by the laser radiation is computed from the fluence rate and the absorption coefficient.

3. STATE ESTIMATION PROBLEM

The direct (forward) problem associated with the physical problem described above consist in determining the fluence rate distribution and the temperature distribution in the tumor and skin tissues, from the knowledge of initial and boundary conditions, heat sources, geometry, optical and thermophysical properties. The inverse problem addressed in this work aims at the estimation of the spatial distribution of the fluence and of transient temperature field in the tumor and skin tissues, by accounting for uncertainties on the mathematical model of the physical problem and by assuming local temperature measurements available at one location inside the domain.

Inverse problems in which the unknowns are time-dependent are referred to as non-stationary inverse problems (Kaipio and Somersalo, 2004). In fact, it turns out necessary in several applications to obtain estimates of some variables from measurements obtained sequentially, in order to monitor a given process. In these situations, non-stationary inverse problems may be written in the form of evolution and observation stochastic models and referred to as a state estimation problem (Kaipio and Somersalo, 2004).

The objective of the state estimation problem is to obtain information about the state vector, $\mathbf{x}_k$, based on the evolution and observation models. Once the state evolution and observation models are defined, the solution of the state estimation problem can be obtained with Bayesian filters. The most known Bayesian filters are the Kalman filter and its extensions, which give good results under some restrictive conditions on the evolution and observations models. Particle filters, or sequential Monte Carlo are more general, and can be applied to non-linear evolution and observation models with non-Gaussian noises (Arulampalam et al., 2001). The particle filters used in this work are described next.

3.1 The Sampling Importance Resampling Filter (SIR)

In the SIR algorithm, the importance density $\pi\left(\mathbf{x}_k^i \mid \mathbf{x}_{k-1}^i\right)$ is chosen as the prior density. Since the importance density is independent of the information conveyed by the measurements $\mathbf{z}_k^{meas}$, the state space is explored without any information of the measurements. Hence, this filter can be inefficient and sensible to outliers (Arulampalam et al., 2001). Such algorithm can be summarized in the steps presented in Table 1, as applied to the system evolution from t_{k-1} to t_k (Arulampalam et al., 2001, Ristic et al., 2004).

Table 1 Sampling importance resampling algorithm (Arulampalam et al., 2001, Ristic et al., 2004).

Step 1
For i = 1,...,N draw new particles $\mathbf{x}_k^i$ from the prior density $\pi(\mathbf{x}_k\|\mathbf{x}^i_{k-1})$ and then use the likelihood density to calculate the corresponding weights $w^i_k = \pi(\mathbf{z}_k\|\mathbf{x}_k^i)w^i_{k-1}$.
Step 2
Calculate the total weight $t = \Sigma_i w^i_k$ and then normalize the weights; that is, for i = 1,...,N let $w^i_k = t^{-1}w^i_k$.
Step 3
Resample the particles as follows: Construct the cumulative sum of weights (CSW) by computing $c_i = c_{i-1} + w^i_k$ for i = 1,...,N, with $c_0 = 0$ Let i = 1 and draw a starting point u_1 from the uniform distribution U[0,N^{-1}] For j = 1,...,N Move along the CSW by making $u_j = u_1 + N^{-1}(j-1)$ While $u_j > c_i$ make $i = i + 1$ Assign sample $\mathbf{x}_k^j = \mathbf{x}_k^i$ Assign uniform weights to the samples $w^j_k = N^{-1}$

3.2 The Auxiliary Sampling Importance Resampling Filter (ASIR)

The Auxiliary Sampling Importance Resampling filter was introduced by Pitt and Shepard, (1999) as a variant of the SIR filter, in which an attempt is made to overcome the loss of diversity by performing the resampling step at time

t_{k-1}, with the available measurement at time t_k (Arulampalam et al., 2001, Ristic et al., 2004). In other words, the idea is to mimic the availability of the optimal importance density $\pi\left(\mathbf{x}_k^i \mid \mathbf{x}_{k-1}^i, \mathbf{z}_k\right)$ (Särkka, 2013). The resampling is based on some point estimate $\boldsymbol{\mu}_k^i$ that characterizes $\pi\left(\mathbf{x}_k^i \mid \mathbf{x}_{k-1}^i\right)$, which can be the mean of $\pi\left(\mathbf{x}_k^i \mid \mathbf{x}_{k-1}^i\right)$ or simply a sample of $\pi\left(\mathbf{x}_k^i \mid \mathbf{x}_{k-1}^i\right)$. If the state evolution model noise is small, then $\pi\left(\mathbf{x}_k^i \mid \mathbf{x}_{k-1}^i\right)$ is generally well characterized by $\boldsymbol{\mu}_k^i$, so that the weights w_k^i are more even and the ASIR algorithm is less sensitive to outliers than the SIR algorithm. On the other hand, if the state evolution model noise is large, then the single point estimate $\boldsymbol{\mu}_k^i$ in the state space may not characterize well $\pi\left(\mathbf{x}_k^i \mid \mathbf{x}_{k-1}^i\right)$ and the ASIR algorithm may not be as effective as the SIR algorithm. The ASIR algorithm can be summarized in the steps presented in Table 2, as applied to the system evolution from t_{k-1} to t_k (Arulampalam et al., 2001, Ristic et al., 2004).

In this work, the state variables are given by the transient temperatures and the fluence rate at the discrete points inside the domain that coincide with the center of finite volumes used in the discretization of the direct problem. Note that the fluence rate is treated as a state variable although not being time dependent, so that inference on its distribution and the distribution of the transient temperature field are obtained simultaneously. The Sampling Importance Resampling (SIR) and the Auxiliary Sampling Importance Resampling (ASIR) versions of the particle filter described in Tables 1 and 2, respectively, are used for the estimation of the posterior probability distribution $\pi\left(\mathbf{x}_k \mid \mathbf{z}_{1:k}\right)$.

Table 2 Auxiliary Sampling importance resampling algorithm (Arulampalam et al., 2001, Ristic et al., 2004).

Step 1
For $i = 1,\ldots,N$ draw new particles $\mathbf{x}_k^i$ from the prior density $\pi(\mathbf{x}_k \mid \mathbf{x}^i_{k-1})$ and then calculate some characterization $\boldsymbol{\mu}_k^i$ of $\mathbf{x}_k$, given $\mathbf{x}_{k-1}^i$. Then use the likelihood density to calculate the corresponding weights $w^i_k = \pi(\mathbf{z}_k \mid \boldsymbol{\mu}_k^i) w^i_{k-1}$.
Step 2
Calculate the total weight $t = \Sigma_i w^i_k$ and then normalize the weights; that is, for $i = 1,\ldots,N$ let $w^i_k = t^{-1} w^i_k$.
Step 3
Resample the particles as follows: Construct the cumulative sum of weights (CSW) by computing $c_i = c_{i-1} + w^i_k$ for $i = 1,\ldots,N$, with $c_0 = 0$ Let $i = 1$ and draw a starting point u_1 from the uniform distribution U$[0,N^{-1}]$ For $j = 1,\ldots,N$ Move along the CSW by making $u_j = u_1 + N^{-1}(j-1)$ While $u_j > c_i$ make $i = i + 1$ Assign sample $\mathbf{x}_k^j = \mathbf{x}_k^i$ Assign sample weights $w^j_k = N^{-1}$ Assign parent $i^j = i$
Step 4
For $j = 1,\ldots, N$ draw particles $\mathbf{x}^j_k$ from the prior density $\pi(\mathbf{x}_k \mid \mathbf{x}^{i^j}_{k-1})$, using the parent i^j, and the use the likelihood density to calculate the corresponding weights $w^j_k = \pi(\mathbf{z}_k \mid \mathbf{x}^j_k) / \pi(\mathbf{z}_k \mid \boldsymbol{\mu}_k^{i^j})$.
Step 5
Calculate the total weight $t = \Sigma_j w^j_k$ and then normalize the weights; that is, for $j = 1,\ldots, N$ let $w^j_k = t^{-1} w^j_k$.

4. RESULTS

The simulations results presented in this paper were carried out by assuming the optical and thermophysical properties given in table 3 for the skin tissues (Çetingül and Herman, 2010, 2011, Bashkatov et al., 2011). Table 3 also shows the respective thickness of each layer. The optical properties of the tumour loaded with gold nanorods (are shown in table 4 and were calculated by assuming a concentration $3\text{x}10^{15}$ $1/\text{m}^3$. It is assumed here that only the absorption and the scattering coefficients are affected by the inclusion of the nanoparticles. The first and second moment of Fresnel reflection coefficient for the air-tissue interface, with the tissue refractive index n_t=1.3, are given as

0.565 and 0.429, respectively (Prahl, 1988). The initial distribution of temperature in the skin model is obtained from the steady-state version of the bioheat transfer problem given by equations 5, by considering a heat transfer coefficient h_c= 10 W/(m^2.K) at the skin surface, while the heat transfer coefficient to deeper tissues was set to h_{int}=50 W/(m^2.K) (Dombrovsky et al., 2012). For the hyperthermia treatment of the subcutaneous tumor, assumed loaded with nanoparticles, use is made of collimated plane laser beam (λ = 800 nm, 2 W/cm^2). The irradiation time was set to 20 s under constant illumination in order to reduce the computation cost of the inverse problem solution. However we note that, it is common to use pulsed laser irradiation for tens of minutes (Dombrovsky et al., 2012). In order to avoid an overheating of the skin surface, a heat transfer coefficient h_c= 100 W/(m^2.K) to a medium at T=35 °C was considered for radial positions smaller than the tumor radius, while the heat transfer coefficient for larger radial positions was set to h_c=10 W/(m^2.K) (Dombrovsky et al., 2012). For the solution of both radiation and bio-heat transfer problems, a finite volume code based on the alternating direction implicit method (ADI) was developed (Lamien et al., 2015).

Table 3: Thermophysical and optical properties (Çetingül and Herman, 2010, 2011, Bashkatov et al., 2011)

Tissue	Epidermis	Tumor	Dermis	Fat	Muscle
Thickness, (mm)	0.1	0.75	1.5	2	8
ρ (kg/m^3)	1200	1030	1200	1000	1085
c_p (J/kg K)	3589	3852	3300	2674	3800
k (W/m K)	0.235	0.558	0.445	0.185	0.51
Q_{met} (W/m^3)	0	3680	368.1	368.3	684.2
ω_b (1/s)	0	63x10^{-4}	2x10^{-4}	10^{-4}	27x10^{-4}
κ (1/m)	35	122	122	108	54
σ_s (1/m)	21270	22500	22500	20200	6670

Table 4: Optical properties of the tumor containing gold nanorods

Concentration of nanoparticles (m^{-3})	3x10^{15}
κ (m^{-1})	177.02
σ_s (m^{-1})	22503.46

For the solution of the state estimation problem, uncertainties in the evolution model of temperature were assumed additive, Gaussian, with means given by their respective deterministic solutions and with constant standard deviation of 0.5 °C. The evolution model of fluence rate distribution was defined in the form of a random walk, with Gaussian noise of zero mean and a standard deviation of 1% of the deterministic value of the fluence rate. Transient temperature measurements at the position (r = 0.5 mm, z= 0.7 mm), taken at a rate of one measurement every 1 s, were assumed available for the inverse analysis. The measurement errors are also assumed Gaussian, with zero mean and a constant standard deviation of 0.5 °C. In order to avoid an inverse crime, different meshes were used for the solution of the forward model for both simulated temperature measurements generation and state estimation. Both SIR and ASIR filters were used for the solution of the state estimation problem with N= 100 and N = 250 particles. The accuracies of the estimates obtained with the aforementioned filters were compared in terms of the root mean square error between the estimated temperatures and the exact ones, which is given by:

$$RMS = \sqrt{\frac{\sum_{k=1}^{M}\left(T_{i,j}^{k} - T_{exa,i,j}^{k}\right)^2}{M}} \tag{6}$$

where $T_{i,j}^{k}$ and $T_{exa,i,j}^{k}$ represent the estimated and exact temperature at the finite volume node (i,j) and at the time instant t_k, respectively and M is the number of time steps.

Figures 2 present the estimated and exact transient temperatures at the sensor location obtained with both SIR and ASIR filters, for both N=100 and N=250 particles. The confidence bounds of the estimated temperature were also included in these figures. As it can be seen in these figures, accurate estimates of the temperatures were obtained, with the estimated temperatures being generally closer to the exact one than the simulated temperature measurements. One should note also in these figures that, the increase of the number of particles from N=100 to N=250 has a small effect on the confidence bounds of the estimated transient temperatures; that is the confidence bounds have converged with N=100 particles.

Table 5 shows the performance of the SIR and ASIR filters in terms of RMS errors of the temperature, for both N=100 and N=250 particles. As it can be noticed in this table, the RMS errors at the positions examined generally decreases with the increase of the number of particles, for both SIR and ASIR filters. In the other hand, one can note that the SIR filter has presented lowers RMS errors for both N=100 and N=250 particles. Furthermore, by comparing the computation cost of the two filters one can note that, the computation cost of the ASIR filter is as twice the one needed for the SIR filter (See Table 6). This is due to the fact that in the ASIR filter the state evolution model is performed twice (see Table 2).

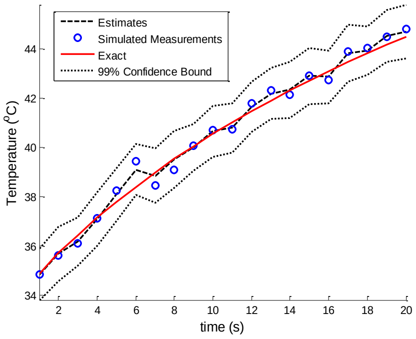

(a)

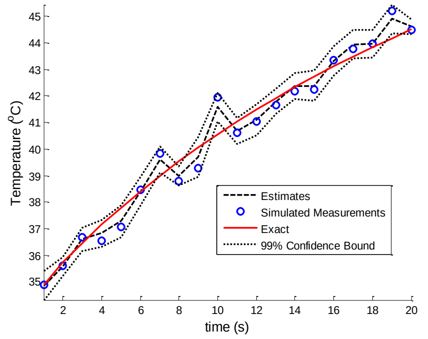

(c)

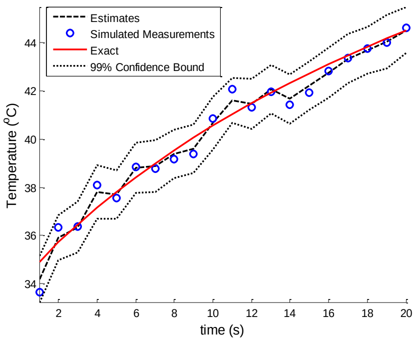

(b)

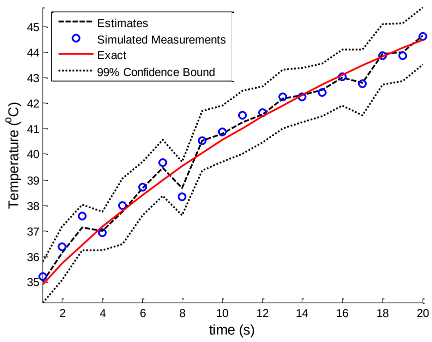

(d)

Fig. 2 Comparison of the estimated and exact transient temperature variations with the temperature measurements at the sensor position (r = 0.5 mm, z = 0.7 mm) (left) SIR filter for N=100 particles (a), for N=250 particles (b); (right) ASIR filter for N=100 particles (c), for N=250 particles (d)

Table 5 RMS errors of the temperature at different positions inside the domain

	Position / Number of Particles	p_1= (0,5; 0.7) (mm)	p_2=(6; 0,7) (mm)	p_3=(0 ; 3) (mm)	p_4=(0 ; 0,7) (mm)
SIR filter	N=100	0.3135	0.1443	0.1259	0.2149
	N=250	0.3203	0.1058	0.0834	0.1774
ASIR filter	N=100	0.3743	0.1988	0.1718	0.2377
	N=250	0.3598	0.1694	0.1387	0.1823

Table 6 Computational time of the inverse problem solution

Particle filter Algorithm	**Number of Particles**	**CPU time**
SIR	100	26 min 52 s
SIR	250	63 min 57 s
ASIR	100	46 min 57 s
ASIR	250	113 min 23 s

5. CONCLUSIONS

This work has dealt with the comparison of two particle filter algorithms, namely the Sampling Importance Resampling (SIR) filter and the Auxiliary Sampling Importance Resampling (ASIR) filter, for the solution of the inverse state estimation problem of spatial and temporal distribution of temperature resulting from the hyperthermia treatment of a subcutaneous tumor. The results obtained clearly demonstrate the ability of these algorithms in providing accurate estimates of the spatial and temporal temperature distributions, under model uncertainties and noisy measurements. Furthermore, it was shown, for both particle filter algorithms, that the increase of the number of particles improves the accuracy of the estimates. Moreover, for the given state estimation problem, the SIR filter provides reasonably good results with half of the computational time required by the ASIR filter.

6. ACKNOWLEDGEMENTS

The authors are thankful for the support provided by CNPq, CAPES and FAPERJ, Brazilian agencies for the fostering of science.

7. REFERENCES

Arulampalam, M. S., Maskell, S., Gordon, N., et al., 2001, ‘’A Tutorial on Particle Filters for Online Nonlinear/Non-Gaussian Bayesian Tracking’’, IEEE Transactions on Signal Processing, Vol. 50, No 2, pp. 174-188.

Bashkatov, A.N., Genina, E.A., Tuchin, V.V., 2011, ‘’Optical Properties of Skin, Subcutaneous, and Muscle Tissues: A Review”, J. Innov. Opt. Health Sci. Vol. 4, No, 1, pp. 9-38.

Bayatoziglu, T., Kheradmand, S., Tullius, K. T., 2013, ‘’An Overview of Nanoparticle Assisted Laser Therapy’’, Int. J. of Heat and Mass Transf, v. 67, pp. 469-486.

Carp, A. S., Prahl, A.S, Venugopalan, V., 2004, ‘’Radiative Transport in the Delta-P1 Approximation: Accuracy of Fluence Rate and Optical Penetration Depth Predictions in Turbid Semi-infinite Media’’ Journal of Biomedical Optics, Vol. 9, No. 3, pp. 632-647.

Çetingül, M. P., Herman, C., 2010, ‘’A Heat transfer model of skin tissue for the detection of lesions: sensitivity analysis’’, Physics in Medicine and Biology, Vol. 55, No. 19, pp. 5933-5951.

Çetingül, M. P., Herman, C., 2011, ‘’Quantification of the thermal signature of a melanoma lesion’’, Int. J. Therm. Sci., Vol. 50, No. 4, pp. 421-431.

Chatterjee, D., Krishnan, S., 2013, ‘’Gold nanoparticle – mediated hyperthermia in cancer therapy,’’ In S. Cho and S Krishnan, Eds., Cancer Nanotechnology, Boca Raton, CRC Press, pp. 171-182.

Dombrovsky, L. A., Timchenko, V., Jackson, M., 2012, ‘’Indirect Heating Strategy for Laser Induced Hyperthermia: An Advanced Thermal Model’’, Int. J. of Heat and Mass Transf, v. 55, pp. 4688–4700.

Dos Santos, I., Haemmerich, D., Schutt D, da Rocha, A.F., Menezes, L.R., 2009, ‘’Probabilistic Finite Element Analysis of Radiofrequency Liver Ablation Using the Unscented Transform,’’ Phys. Med. Biol., 54, pp.627-640.

Doucet, A., Freitas, N., Gordon, N., 2001, ‘’ Sequential Monte Carlo Methods in Practice’’, Springer, New York.

Greef, D.M., Kok, H.P., Correia, D., Borsboom, P.P, Bel, A., Crezee, J., 2011, ‘’Uncertainty in Hyperthermia Treatment Planning: The Need for Robust System Design’’, Phys. Med. Biol., 56, pp.3233-3250.

Hurwitz, M., 2013, ‘’Principles and Application of Hyperthermia Combined with Radiation, ’’ In S. Cho and S Krishnan, Eds., Cancer Nanotechnology, Boca Raton, CRC Press, pp. 25-36.

Kaipio, J. P. and Somersalo, E., 2004, ‘’Statistical and Computational Inverse Problems’’, Applied Mathematical Sciences 160, Springer-Verlag.

Lamien, B., Orlande, H.R.B., 2014, ‘’State Estimation Problem in Hypertthermia Treatment of Tumors Loaded with Nanoparticles, Proceedings of the 15th International Heat Transfer Conference, August 10-15, 2014, Kyoto, Japan.

Lamien, B., Orlande, H.R.B., Elicabe,G., 2015 "Laser Heating of Soft Tissue Phantoms with an Inclusion Loaded with Plasmonic Nanoparticles", International Journal of Micro-Nano Scale Transport, submitted.

Pitt, M. Sheard, N., 1999, ‘’Filtering via Simulation: Auxiliary Particle Filters’’, Journal of American Statistical Association, v. 94, n. 446, pp. 590-599

Prahl, S. A., 1988, ‘’Light Transport in Tissue’’, Doctoral Dissertation, The University of Texas, Austin.

Ristic, B., Arulampalam, S., Gordon, N., 2004, ‘’Beyond the Kalman Filter’’, Artech House, Boston.

Särkka, S., 2013, Bayesian Filtering and Smoothing, Cambridge University Press.

Star W.M., 2011, “Diffusion Theory of Light Transport’’. In Welch, A. J., Van Gemert, J.C.M. Eds, Optical-Thermal Response of Laser irradiated Tissue, 2 ed., Dordrecht Heidelberg London New York, Springer.

8. RESPONSIBILITY NOTICE

The authors are the only responsible for the printed material included in this paper.